The North African Journal of Scientific Publishing (NAJSP)
مجلة شمال إفريقيا للنشر العلمي (NAJSP)
E-ISSN: 2959-4820
Volume 2, Issue 4, October - December 2024
Page No: 33-40
Website: https://najsp.com/index.php/home/index
SJIFactor 2024: 5.49 معامل التأثير العربي (AIF) 2023: 0.63 ISI 2024: 0.696

An X-Ray Diffraction Study of Au Thin Film Microstructures by Scherrer Equation and Strain Size Plot Methods

Maryam Akhwater *
* Department of physics, Faculty of art and science – Almarj, University of Benghazi, Libya

دراسة حيود الأشعة السينية للهياكل الدقيقة لأغشية الذهب الرقيقة بواسطة معادلة شيرورونموذج مخطط حجم الإجهاد

* مريم اخويطر
قسم الفيزياء، كلية الآداب والعلوم - المرج، جامعة بنغازي، بنغازي، ليبيا

*Corresponding author: maryam.akhwater@uob.edu.ly

Received: July 07, 2024	Accepted: September 08, 2024	Published: October 10, 2024

Abstract:
The X-ray diffraction technique is an easy and powerful tool for investigating the crystal structure of nanocrystalline bulk materials, which play a key role in a wide range of potential applications. In this paper, Au thin films were deposited by the radio frequency sputtering method onto Si substrates and then were characterized using the X-ray diffraction technique (XRD). The XRD patterns confirmed the crystallinity of Au thin films with FCC structure. The peak broadening analysis was applied to estimate the microstructural properties, including crystallite sizes and lattice strains, using Debye Scherrer equation-based methods, including linear straight-line, linear straight-line passing through the origin, and the average size of the crystal. In addition, the Monshi–Scherrer equation model and the size strain plot (SSP) method were also used. The obtained findings showed that the estimated crystalline size of the Au thin films by the proposed models was highly intercorrelated. The microstructural parameters evaluated from the suggested methods were compared with previously published HR-TEM, AFM, and SEM results. Apart from the linear straight-line model of the Scherrer equation, all results of the crystallite size for deposited thin films were accurate with significant agreement to previously published TEM data.

Keywords: Au Thin Films; Crystallite Size; X-Ray Diffraction; Modified Scherrer Method; Strain Size Plot.

الملخص
تعد تقنية حيود الأشعة السينية أداة سهلة وقوية لفحص البنية البلورية للمواد الكبيرة البلورية النانوية، والتي تلعب دورًا رئيسيًا في مجموعة واسعة من التطبيقات المحتملة. في هذا البحث، تم ترسيب أغشية الذهب الرقيقة بطريقة الرش بالترددات الراديوية على ركائز السيليكون ثم تم دراستها باستخدام تقنية حيود الأشعة السينية *(XRD)*. أكدت أنماط حيود الأشعة السينية تبلور أغشية الذهب الرقيقة بهيكل *(FCC)*. تم تطبيق تحليل اتساع القمة لتقدير خصائص البنية المجهرية، بما في ذلك أحجام البلورات والسلالات الشبكية، باستخدام معادلة شيرور *(Debye Scherrer)* القائمة على النماذج الاتية: الخط المستقيم الخطي، والخط المستقيم الخطي الذي يمر عبر الأصل، ومتوسط حجم البلورة. بالإضافة إلى ذلك، تم أيضًا استخدام نموذج معادلة موشي- شيرور *Monshi-Scherrer* وطريقة مخطط حجم الإجهاد *(SSP)*. لقد أظهرت النتائج

التي تم الحصول عليها أن الحجم البلوري التقديري لأغشية الذهب الرقيقة بواسطة النماذج المقترحة كان متقاربا للغاية. تمت مقارنة معاملات البنية البلورية المجهرية التي تم تعيينها باستخدام الطرق المقترحة مع النتائج المنشورة سابقًا لتقنيات المجهر الالكتروني عالي الدقة *(HR-TEM)*ومجهر القوة الذرية *(AFM)* ومجهرالمسح الالكتروني*(SEM)* . باستثناء نموذج الخط المستقيم الخطي لمعادلة شيرور، كانت جميع نتائج الحجم البلوري لأغشية الذهب الرقيقة في توافق جيد مع بيانات المجهر الالكتروني عالي الدقة المنشورة مسبقًا.

الكلمات المفتاحية: اغشية الذهب الرقيقة، الحجم البلوري، حيود الأشعة السينية، طريقة شيرور المعدلة، مخطط حجم الإجهاد.

1. Introduction

Solid crystalline nanomaterials have been the focus of today's nanotechnology research due to their prominent performance in electronics, optical, electrochemical, electromechanical and photonics applications. However, the functionality of these nanomaterials is eventually dictated by the capability to control their fundamental physical and structural properties on the nanosized scale. Compared to the bulk structure, nanomaterials in the typical range between 1 and 100 nm have shown unique size-dependent characteristics [1]. Therefore, it is critical to initially evaluate the crystallite size for investigating optical [2], electrical and magnetic [3], structural [4], photocatalytic [5], and mechanical properties [6] of these nanocrystalline materials. In addition, the bandgap energy of semiconductor materials was reported to be strongly dependent on the material crystallinity.

Hence, the largest crystallite size provided the lowest bandgap energy and vice versa [2]. Nano-sized Au particles have drawn considerable attention in large-scale industrial and scientific applications because of their remarkable catalytic characteristics [7]. Bulk Au has been considered as an inert metal in catalysis however, when its dimensions are reduced to the nanometre scale, Au acts as an excellent catalyst [8]. These small Au particles show unique catalytic activity, which could be employed in several applications ranging from nanocatalysis to bio-detectors and advanced drug delivery platforms [9]. It has been reported that the catalytic activity of Au nanoparticles can be tuned by their particle size [10], therefore controlling the crystallite size would enhance their catalytic properties.

There have been many techniques, such as Brunauer Emmett Teller (BET), light scattering, scanning electron microscopy (SEM), transmission electron microscopy (TEM), and XRD, which were used to investigate the crystallinity of nanomaterials and measure the structural parameters including the crystallite size and lattice strain. However, the first and most used technique is XRD, which has been in use in two fundamental scopes for the fingerprint characterisation of crystalline materials and the identification of their composition [11]. Such a technique is performed based on the elastic scattering of electrons, which is the variation of the direction of electromagnetic waves without energy loss. Each crystal lattice has a uniform, ordered array of atoms with high atomic density planes, which comprise high electron density. When a monochromatic beam of X-ray photons falls onto crystal planes, scattering will occur, and maximal diffraction may happen if the scattered photons interfere with each other, and subsequently, one diffracted line will take place for each set of the crystal planes [11]. In general, XRD gives a plot of Intensity versus 2θ, which shows a signature peak of the phases existing in the sample. Comparison of this signature peak with standard reference patterns, the required characteristics can be addressed in the sample [11].

In addition, based on X-ray peak broadening, two main elastic properties, including crystallite size and lattice strain, can be evaluated. The crystallite size, which is a measure of the size of a coherently diffracting domain, is not usually the same as the particle size because of the existence of polycrystalline aggregates [12]. Lattice strain is released as a result of crystal imperfections, such as lattice dislocations, grain boundary, triple junction, contact or sinter stresses, stacking faults, and coherency stresses [13]. There are many approaches to measuring these microstructural parameters of crystalline materials, however, one crucial point is to apply efficient techniques that could precisely estimate these properties. Hence, the present study aims to demonstrate and compare the crystallite size and lattice strain of Au thin films obtained from XRD peak broadening and estimated using various methods, including the Scherrer equation (three models), Monshi–Scherrer equation, and the size strain plot Method (SSP).

2. Material and Methods

Silicon (p-type, (100)) substrates with a surface of 1 × 1 cm^2 were ultrasonically cleaned by acetone and isopropanol for 20 min each to clear away surface contamination and then were kept in a deionized water bath for 15 min. Silicon substrates were blown dry with nitrogen gas and baked on a hotplate at 150 ^{0}C for 10 min to eliminate any adsorbed moisture. A thin Au film (7 nm) was then deposited onto silicon substrates by radio frequency sputtering technique. In addition, to investigate the structure properties of the Au thin films, XRD with Cu-Kα X-ray radiation having a characteristic wavelength of 0.15418 nm was applied. The scan speed of 2^0/min was performed from 10^0 to 90^0. The XRD patterns were analysed through the X'Pert HighScore software with the assistance of OriginPro data analysis software to determine the crystallite size and micro-strain of Au thin films. X'Pert HighScore software is widely used to identify the reference pattern of XRD data by comparing the measured peaks to the software database and selecting the most potential candidate for the measured diffraction patterns.

3.Results and Discussion

All diffraction peaks can confirm the face-centred cubic structure of Au according to the standard data of the Joint Committee on Powder Diffraction Standards (JCPDS), having card no.04-0784 of Au nanocrystal [14] and (American Mineralogist Crystal structure database, Codes No. 0013108) [15]. The XRD pattern of Au thin films is shown in Figure 1. It was observed that the intensity of peaks was sharp and narrow, indicating that Au thin films showed high crystallinity with good phase purity. In the following subsections, these diffraction data were used to evaluate the crystalline size and the lattice strain of Au thin films using various models based on the Scherrer equation, Monshi–Scherrer equation, and the SSP.

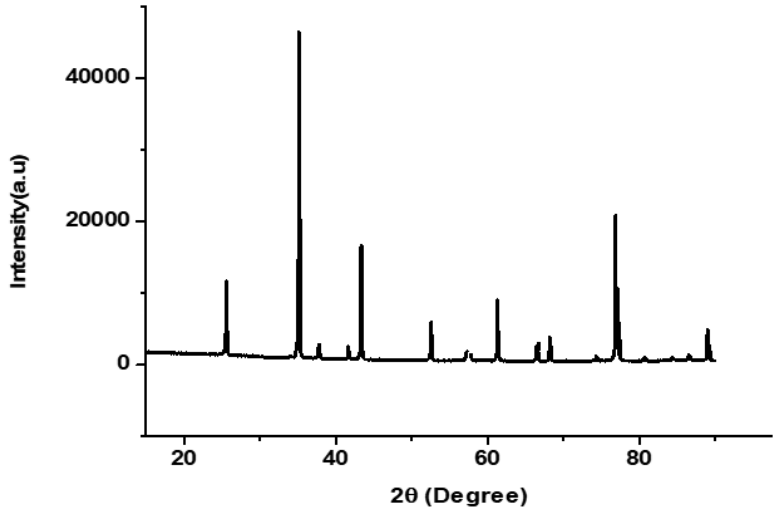

Figure 1: The XRD pattern of Au thin films.

3.1 Scherrer equation models

All diffraction peaks are considered and the full width at half maximum (FWHM) of the peaks was used to estimate the crystallite size using the correlation between the size of the crystal and XRD width. Thus, the crystallite size was determined by Debye-Scherrer formula as follows:

$$D=k\lambda/\beta_D\cos\theta \quad (1)$$

Where λ is the wavelength of the X-rays used (0.15405 nm), D is the crystallite size, k is the Scherrer constant (≈ 0.89), θ is the diffraction angle, and β_D is the FWHM; in radians. The breadth of diffraction peaks is a contribution of both the instrument and the tested sample. For a precise measurement of crystallite size and strain broadening, the instrumental broadening (β_D) must be accounted therefore, it is required to assemble a diffraction pattern from the line broadening of samples, such as silicon or lanthanum hexaboride [16]. Those samples must be measured using the same optics that are used to analyse the tested samples. The instrument-corrected broadening corresponding to the diffraction peaks was estimated using the following equation (2):

$$\beta^2_D = [\beta^2_m + \beta^2_i] \quad (2)$$

Herein, β_m is the measured broadening and β_i is the instrumental broadening. Many publications applied the Scherrer equation only for the strong peaks and neglected other weak peaks. In the current work, three suggested models of the Scherrer equation namely, the model of a straight line, the model of a straight line passing the origin, and the average model, were performed to calculate the crystal size and microstrain of Au thin films. Furthermore, the β_D values of all diffraction peaks and the position of the peaks are listed in Table.1.

Table 1: The microstructure parameters of Au thin films extracted from the XRD pattern.

2θ (Deg)	β_D (Deg)	θ (Deg)	Cos θ (Deg)	1/Cos θ (Deg)	Ln (1/Cos θ) (Deg)	β_D (Rad)	Ln(β_D) (Rad)	d-spacing [nm]
25.574	0.40	12.78	0.975	1.025	0.025	0.0069	-4.9762	0.3480
35.145	0.60	17.57	0.953	1.049	0.047	0.0104	-45659	0.2551
38.392	2.80	19.19	0.944	1.059	0.057	0.0487	-3.0221	0.2342
41.670	0.40	20.83	0.934	1.071	0.068	0.0069	-4.9762	0.2165
43.348	0.52	21.67	0.929	1.076	0.073	0.009	-4.7105	0.2085
52.545	0.64	26.27	0.896	1.116	0.109	0.0111	-4.5008	0.1740
57.149	1.12	28.57	0.878	1.138	0.129	0.0194	-3.9424	0.1610
61.295	0.72	30.64	0.860	1.163	0.151	0.0125	-4.3820	0.1511
66.511	0.64	33.25	0.836	1.196	0.178	0.0111	-4.5008	0.1404
68.202	0.64	34.10	0.828	1.207	0.188	0.0111	-4.5008	0.1373
77.224	0.72	38.61	0.781	1.28	0.246	0.0125	-4.3820	0.1234
80.763	0.90	40.38	0.761	1.314	0.273	0.0156	-4.1605	0.1189
88.980	0.76	44.49	0.713	1.40	0.336	0.0132	-4.3275	0.1099

3.1.1 Model of a straight line

In this model, all diffraction peaks were included and by rearranging equation (1), it can be written as Equation (3):

$$\cos\theta = k\lambda/D.\ 1/\ \beta_D \qquad (3)$$

Hence, in Equation (3) a plot is performed with $1/\ \beta_D$ along the *X*-axis and $\cos\theta$ along the *Y*-axis as shown in Figure 2. According to the linear fit of the data, the crystalline size was calculated from the slope of the plot, which is equal to $k\lambda/D$. Thus, the measured crystallite size of Au thin films was 979 nm. Furthermore, it showed a poor linear fitting value (R^2=0.08), which suggests that the Scherer equation requires some modifications to precisely estimate an accurate crystallite size. The diffraction peak broadening is affected by the lattice strain contributions which should be taken into account for more validity and accuracy of the crystallite size. The measurement of crystallite size calculated from the slope of a straight line model is inaccurate and unacceptable, as it should be in the scale of (1-100 nm). Therefore, to improve the accuracy of the Scherrer equation, it is advised to make the line passing through its respective origin.

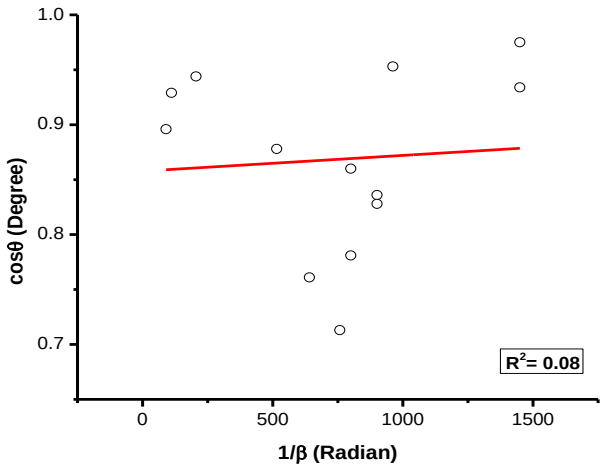

Figure 2: The linear plot of the model of a straight line for Au thin films.

3.1.2 Model of the straight line passing the origin

In this model, Equation (5) was applied to perform the linear fitting which passes through the origin and produces an acceptable slope for estimation of crystallite size [17]. The linear fitting equation can be written as following:

$$Y = M.X \tag{4}$$

If Y_i represents the intensity of the ith point and X_i its related 1/ β_D value, the slope using the least-squares method can be given as,

$$M = \frac{\sum_i Y_i X_i}{\sum_i X_i^2} \tag{5}$$

Thus, using the slope values obtained from Equation (5) for all of the diffraction peaks the crystallite size was 18.28 nm. It is obvious that the result of a least square method for a straight line going through the origin is more valid and accurate.

3.1.3 Average model in Scherrer equation

In this model, the crystallite size was estimated using the average approach according to the Scherrer Equation (1), so after the calculations, the values of crystal size were averaged to be 13.77nm. Comparing the Scherrer equation-based models, it can be concluded that the size of the crystal estimated by a least square method of the linear fit and the average approach was more reasonable than applying the Scherrer equation for all the peaks without any modification. Such differences could be due to the increase of the diffraction angle decreasing the validity of FWHM values [18], whilst adjustment of the Scherrer equation results in minimizing the sources of errors.

3.2 Monshi–Scherrer model

From a theoretical perspective, if there is N different peaks of a particular nanocrystalline material at a specific scale of θ, thus the size of this nanocrystal must be the same for all N peaks. However, from a practical point of view, it was found that every single peak gives a different crystallite size as systematic errors are not avoidable in the Scherrer equation. Therefore, to minimize error and provide the exact crystal size for all peaks (or any number of selected peaks) in a specific material, some adjustments related to the peak position and the peak broadening were performed [18]. Monshi et al. [18] proposed a modified Scherrer equation, which is known as the Monshi–Scherrer equation, to address this issue. So, Equation (6) can be rearranged as,

$$\beta_D = \frac{k\lambda}{D}\frac{1}{\cos\theta} \tag{6}$$

To produce a decrease of errors in the estimated results, the logarithm of both sides of Equation (6) is applied, therefore Equation (7) can be written in a logarithmic form as,

$$Ln\ \beta_D = Ln\frac{k\lambda}{D} + Ln\frac{1}{cos\ \theta} \tag{7}$$

According to Equation (7), $Ln\ \beta_D$ and $Ln\ (1/Cos\ \theta)$ can be plotted as Y and X axes respectively (see Figure 3), then using the least squares approach to get good linear fitting. The intercept, which is equal to $Ln\ (K\lambda/D)$, can be found, and then the single value of the crystallite size can be calculated from all diffraction peaks by taking the exponential of the intercept. Thus, the estimated size of Au nanocrystals was 11.94nm with a slope value near one, indicating the high validity of the Monshi–Scherrer model.

The findings were in good agreement with the crystallite size of 12.3 nm, 12.5, nm, and 11.8 nm which were extracted using the X-ray diffraction line profile analysis for Au thin films deposited on Si (100), Si (111) and glass substrates, respectively [19]. Moreover, Scherrer-based models, namely the averaged and straight line passing the origin models and the Monshi–Scherrer model were reasonably matched with experimentally estimated size via the TEM technique [20].

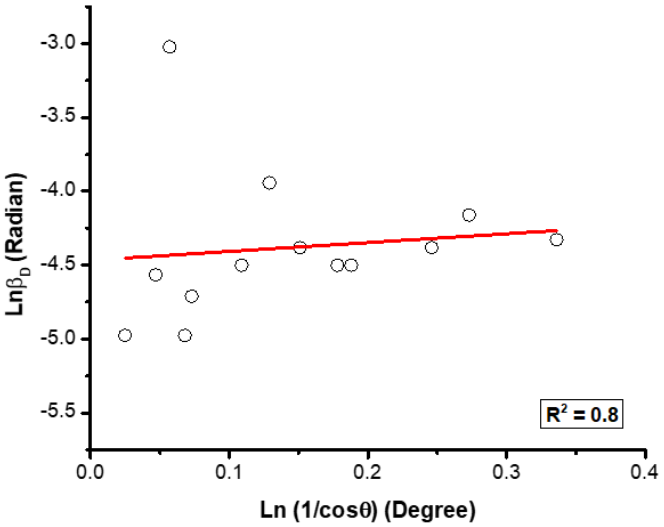

Figure 3: The linear fitting of the Monshi–Scherrer model.

3.3 Size strain plot method (SSP)

SSP is another way to estimate the size of the crystal and the microstrain from the profile of the peak diffraction. In this approach, more significance is considered to data from reflections at low angles, due to larger values of the peak position and the intensity leading to overlapping peaks where the precision is significantly dropped, and the quality is quite low. It was demonstrated that the XRD profile is a contribution of Lorentzian function (crystallite size) and Gaussian function (microstrain) [21]. Hence, the total broadening of SSP can be given as,

$$\beta = \beta_G + \beta_L \tag{8}$$

Where β_L and β_G are the peaks broadening due to Lorentz and Gaussian functions, respectively. The introduced equation of the SSP method is given as,

$$(d_{hkl}.\beta_{hkl}.cos\theta)^2 = \frac{k\lambda}{D}.(d_{hkl}^2.\beta_{hkl}.cos\theta) + \frac{\varepsilon^2}{4} \tag{9}$$

Based on Table 1, it can plot $(d_{hkl}^2.\beta_{hkl}.cos\theta)$ and $(d_{hkl}.\beta_{hkl}.cos\theta)^2$ for all diffraction peaks along *X* and *Y* axes, respectively. Besides, the crystallite size of Au thin films can be calculated from the slope of the linear fitting of data (see Figure 4). According to Equation (9) the value of the intercept is equal to ($\varepsilon^2/4$), where ε is the lattice strain. Hence, the estimated crystallite size was 15.23 nm and microstrain was 0.0026.

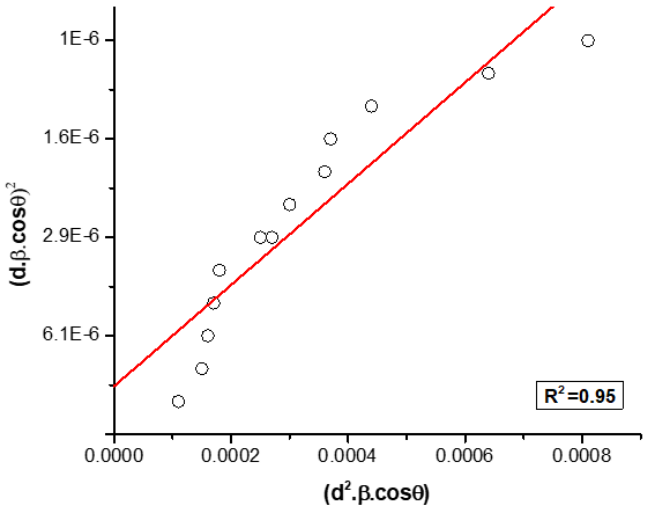

Figure 4: The linear fitting of the SSP model.

The linear correlation (R^2 =0.95) indicates the high validity of the SSP model for estimating the size of the crystal. In addition, the obtained size by SSP was in well matching with the analyses of TEM (D = 18 nm) [22].

4. Conclusion

To summarize, the certainty and accuracy of the crystallite size estimation procedure are significantly critical as this structural feature could highly affect the performance of nanocrystalline material in different applications. In this study, the microstructural properties of Au thin films were characterized using X-ray diffraction line broadening methods. The crystalline phase of Au thin films was confirmed by the XRD pattern according to the standard database. In addition, various applicable models such as the Scherrer equation-based methods, including linear straight-line, linear straight-line passing through the origin, the average size and the Monshi-Scherrer method and the SSP model, were used for the estimation of crystallite size of Au thin films. Apart from the linear straight-line model of the Scherrer equation, all proposed models showed acceptable values of the crystallite size for deposited thin films. Herein, the microstructure of Au thin films was addressed by the X-ray peak breadth methods, and most of the measured crystallite sizes were highly comparable and intercorrelated. XRD analysis is more effective when further integrated with complementary direct methods such as Raman spectroscopy, scanning electron microscopy (SEM), confocal laser scanning microscopy, and TEM. Therefore, these approaches are highly recommended for a more in-depth characterization of the microstructural properties of crystalline materials.

References

[1] Chen, W., Zhang, J.Z. and Joly, A.G., 2004. Optical properties and potential applications of doped semiconductor nanoparticles. Journal of nanoscience and nanotechnology, 4(8), pp.919-947.

[2] Rahman, A., Lalasari, L.H., Sofyan, N., Daneswara, D. and Yuwono, A.H., 2023, May. Investigating the effect of crystallite size on the optical properties of zinc oxide. In AIP Conference Proceedings (Vol. 2538, No. 1). AIP Publishing.

[3] Iqbal, M.J., Yaqub, N., Sepiol, B. and Ismail, B., 2011. A study of the influence of crystallite size on the electrical and magnetic properties of CuFe2O4. Materials Research Bulletin, 46(11), pp.1837-1842.

[4] Yakubovsky, D.I., Arsenin, A.V., Stebunov, Y.V., Fedyanin, D.Y. and Volkov, V.S., 2017. Optical constants and structural properties of thin gold films. Optics express, 25(21), pp.25574-25587.

[5] Nandiyanto, A.B.D., Zaen, R. and Oktiani, R., 2020. Correlation between crystallite size and photocatalytic performance of micrometer-sized monoclinic WO3 particles. Arabian Journal of Chemistry, 13(1), pp.1283-1296.

[6] Slama, C., Jaafar, H., Karouia, A. and Abdellaoui, M., 2021. Diffraction crystallite size effects on mechanical properties of nanocrystalline (Ti0. 8W0. 2) C. Chemistry Africa, 4(4), pp.809-819.

[7] WALLACE, W.T. and WHETTEN, R.L., 2002. Coadsorption of CO and O2 on selected gold clusters: Evidence for efficient room-temperature CO2 generation. Journal of the American Chemical Society, 124(25), pp. 7499-7505.

[8] MEYER, R., LEMIRE, C., SHAIKHUTDINOV, S.K. and FREUND, H., 2004. Surface chemistry of catalysis by gold. Gold Bulletin, 37(1-2), pp. 72-124.

[9] CHOUDHARY, T. and GOODMAN, D., 2002. Oxidation catalysis by supported gold nano-clusters. Topics in Catalysis, 21(1), pp. 25-34.

[10] BERNHARDT, T., HEIZ, U. and LANDMAN, U., 2007. Chemical and catalytic properties of size-selected free and supported clusters. Nanocatalysis. Springer, pp. 1-191.

[11] Jenkins, R., 2000. X-ray techniques: overview. Encyclopedia of analytical chemistry, pp.1-

[12] Ramakanth, K., 2007. Basics of X-ray Diffraction and its Application. IK, New Delhi.

[13] ZHANG, J., ZHANG, Y., XU, K. and JI, V., 2006. General compliance transformation relation and applications for anisotropic hexagonal metals. Solid State Communications, 139(3), pp. 87-91.

[14] Swarthmore, P.A., 1991. Joint Committee on Powder Diffraction Standards Diffraction Data File. JCPDS International Center for Diffraction Data.

[15] Suh, I.K., Ohta, H. and Waseda, Y., 1988. High-temperature thermal expansion of six metallic elements measured by dilatation method and X-ray diffraction. Journal of Materials Science, 23, pp.757-760.

[16] Zak, A.K., Majid, W.A., Abrishami, M.E. and Yousefi, R., 2011. X-ray analysis of ZnO nanoparticles by Williamson–Hall and size–strain plot methods. Solid State Sciences, 13(1), pp.251-256.

[17] Monshi, A. and Messer, P.F., 1991. Ratio of slopes method for quantitative X-ray diffraction analysis. Journal of materials science, 26, pp.3623-3627.

[18] Monshi, A., Foroughi, M.R. and Monshi, M.R., 2012. Modified Scherrer equation to estimate more accurately nano-crystallite size using XRD. World journal of nano science and engineering, 2(3), pp.154-160.
[19] Chen, G., Hui, P., Pita, K., Hing, P. and Kong, L., 2005. Conductivity drop and crystallites redistribution in gold film. Applied Physics A, 80, pp.659-665.
[20] Iqbal, M., Usanase, G., Oulmi, K., Aberkane, F., Bendaikha, T., Fessi, H., Zine, N., Agusti, G., Errachid, E.S. and Elaissari, A., 2016. Preparation of gold nanoparticles and determination of their particles size via different methods. Materials Research Bulletin, 79, pp.97-104.
[21] Balzar, D. and Ledbetter, H., 1993. Voigt-function modeling in Fourier analysis of size-and strain-broadened X-ray diffraction peaks. Journal of Applied Crystallography, 26(1), pp.97-103.
[22] Ogundare, O.D., Akinribide, O.J., Adetunji, A.R., Adeoye, M.O. and Olubambi, P.A., 2019. Crystallite size determination of thermally deposited Gold Nanoparticles. Procedia Manufacturing, 30, pp.173-179.